Optical Interferometry with Quantum Networks

E. T. Khabiboulline,[1,*] J. Borregaard,[1,2] K. De Greve,[1] and M. D. Lukin[1]

[1]*Department of Physics, Harvard University, Cambridge, Massachusetts 02138, USA*
[2]*QMATH, Department of Mathematical Sciences, University of Copenhagen, 2100 Copenhagen Ø, Denmark*

We propose a method for optical interferometry in telescope arrays assisted by quantum networks. In our approach, the quantum state of incoming photons along with an arrival time index are stored in a binary qubit code at each receiver. Nonlocal retrieval of the quantum state via entanglement-assisted parity checks at the expected photon arrival rate allows for direct extraction of the phase difference, effectively circumventing transmission losses between nodes. Compared to prior proposals, our scheme (based on efficient quantum data compression) offers an exponential decrease in required entanglement bandwidth. Experimental implementation is then feasible with near-term technology, enabling optical imaging of astronomical objects akin to well-established radio interferometers and pushing resolution beyond what is practically achievable classically.

High-resolution imaging using large telescope arrays is by now a well-established technique in the microwave and radio-frequency domains [1,2]. Although extending to the optical domain may offer substantial advantages in terms of resolution [3,4], this task is extremely challenging in practice. The requirement of interferometric stabilization at optical wavelengths and the weakness of light sources in this domain have precluded the widespread adoption of optical telescope arrays [5]. Notably, the weaker light intensities make phase-sensitive heterodyne detection infeasible due to vacuum fluctuations [6]; therefore, high-resolution optical telescopes are operated by directly interfering the collected light [7]. Then, the size of the array (and consequently resolution) is ultimately limited by transmission losses between telescope sites.

In this Letter, we propose a new approach to overcome these limitations with networks [8] of quantum memories connected via entanglement. Specifically, we describe a scheme for efficiently determining the optical phase difference between two widely separated receivers. Each detector runs a "quantum shift register," storing incident photon states at a rate that is matched to the inverse detection bandwidth. Then, at the anticipated mean photon arrival rate, the memories are interrogated with entangled pairs to provide information akin to that obtained from a radio interferometer. Employing quantum repeater techniques [9], this approach completely circumvents transmission losses. The resulting increase in baseline to arbitrarily large distances potentially allows for substantial enhancement in imaging resolution [4].

Before proceeding, we note that the use of entanglement to connect remote telescope sites has been proposed previously by means of postselected quantum teleportation of incident optical photons [10]. The key limitation of this visionary proposal is the requirement of an excessive amount of distributed entangled pairs. They must be supplied at a rate similar to the spectral bandwidth of the optical telescope, which is currently not feasible. In the
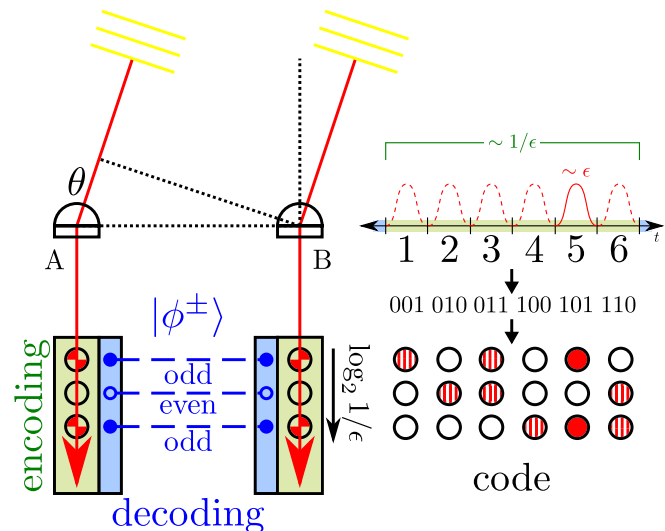

FIG. 1. Overview of basic operation. Light from a distant source is collected at two sites and stored in quantum memory over time bins digitized by detector bandwidth. Both the quantum state and the arrival time of an incident photon are encoded in a binary qubit code. For example, if the photon arrives in the fifth time bin, corresponding to binary representation 101, we store it in a quantum state with flipped first and third qubits at each node. Decoding of the arrival time is accomplished by nonlocal parity checks assisted by entangled pairs, projecting the memories onto a known entangled state. The phase information can then be extracted without directly interfering the signal from the two memories, thus circumventing transmission losses. Network resources scale only logarithmically with source intensity ϵ.

relevant case of weak sources, such that incident photons are rare, the use of quantum memories circumvents this requirement. Under distributed compression, the incoming light is efficiently processed using only $\sim \log_2(1/\epsilon)$ memory qubits and entangled pairs, where $\epsilon \ll 1$ is the mean photon number. Then, the entire loss-free interferometric operation can be realized with modest quantum nodes consisting of about 20 qubits and a distributed entanglement rate in the 200 kHz range. Our proposal realizes an effective event-ready scheme, avoiding the wasteful expenditure of entanglement for vacuum events.

In our protocol, illustrated in Fig. 1, incoming light is stored by flipping stationary quantum bit memories [11] at each telescope site. The storage procedure operates over a time interval set by the detector bandwidth. Multiple qubits are needed to record a photon spread over many time bins. We assume that the light is weak such that most time bins contain vacuum. Consider first a unary encoding with one memory qubit for each time bin. After the single photon is stored, the memories are in a superposition between one site having the excitation versus the other: e.g.,

$$(|000010...\rangle_A |000000...\rangle_B$$
$$+ e^{i\theta} |000000...\rangle_A |000010...\rangle_B)/\sqrt{2},$$

where the memory register corresponds to the time bin. The goal of the interferometer is to extract the relative phase θ. To determine which memory qubits to use for interferometry without collapsing the superposition, the parity of parallel memory registers can be checked with an entangled state per register. Introducing Bell pairs [$|\phi^{\pm}\rangle = (|0,0\rangle \pm |1,1\rangle)/\sqrt{2}$, where $|i\rangle_A |j\rangle_B \equiv |i,j\rangle$], controlled phase (CZ) gates between the memory qubits on either side and the entangled pairs have the following effect:

$$(|0,0\rangle, |1,1\rangle)|\phi^+\rangle \overset{2\times CZ}{\to} (|0,0\rangle, |1,1\rangle)|\phi^+\rangle, \quad (1)$$

$$(|0,1\rangle, |1,0\rangle)|\phi^+\rangle \overset{2\times CZ}{\to} (|0,1\rangle, |1,0\rangle)|\phi^-\rangle. \quad (2)$$

A measurement in the X basis [projecting on the states $|\pm\rangle = (|0\rangle \pm |1\rangle)/\sqrt{2}$] of each qubit in the Bell pair then reveals their parity, from which we can infer the arrival time because the odd-parity register is the one containing the excitation. Its relative phase can be subsequently extracted, e.g., via measurement of one of the qubits in the X basis and the other in a rotated basis to interfere the phase. Similar to a prior scheme [10], the unary code requires one entangled pair for each time bin, implying large consumption for practical bandwidth.

Encoding in binary accomplishes the same task but with a logarithmic scaling of resources. We exploit that only one photon arrives over $M \sim 1/\epsilon$ time bins; i.e., we only have to store one logical qubit per block. Label each time bin $m \in \mathbb{Z}_+$ with its binary representation m_2, and define

logical qubits $|\bar{0}\rangle \equiv |0...0\rangle$ and $|\bar{1}_m\rangle \equiv |m_2\rangle$. For example, the fifth time bin is encoded as $|\bar{1}_5\rangle = |1010...0\rangle$, which is formed from physical qubits at one site. Generally, $\log_2(M+1)$ bits are needed to losslessly encode M possible arrival times plus the vacuum. This encoding is performed by a logical controlled not (CX) gate, which is a product of physical CX gates between the control photonic qubit and target memory qubits specified by the binary representation:

$$|0\rangle(|\bar{0}\rangle, |\bar{1}_j\rangle) \overset{\overline{CX}_m}{\to} |0\rangle(|\bar{0}\rangle, |\bar{1}_j\rangle), \quad (3)$$

$$|1\rangle(|\bar{0}\rangle, |\bar{1}_j\rangle) \overset{\overline{CX}_m}{\to} |1\rangle(|\bar{1}_m\rangle, |\bar{1}_j + \bar{1}_m\rangle). \quad (4)$$

The encoding keeps track of the arrival time of one photon: empty time bins leave the memories unchanged, whereas only the time bin that does contain a photon maps into the quantum memory via the binary code. Decoupling the photonic qubit through an X-basis measurement completes the encoding step but imparts a conditional phase associated with each time bin [12]. This phase must be corrected, requiring knowledge of the time bin when the photon did arrive. The arrival time can be decoded while preserving spatial coherence by applying nonlocal parity checks on qubit pairs in the same register analogously to the case of unary encoding described earlier. For example, if the photon arrived in the fifth time bin, the Bell pairs would be found in the state $|\phi^-\rangle|\phi^+\rangle|\phi^-\rangle|\phi^+\rangle...|\phi^+\rangle$. Because there are $\log_2(M+1)$ qubits per memory, $\log_2(M+1)$ preestablished entangled pairs are also consumed.

Besides identifying the photon arrival time, the parity checks project out the vacuum component of the state. Modeling the astronomical object as a weak thermal source [35,36], the light arriving in each time bin is described by a density matrix [6]

$$\rho_{AB} = (1-\epsilon)\rho_{vac} + \frac{\epsilon(1+|g|)}{2} |\psi_\theta^+\rangle\langle\psi_\theta^+|$$
$$+ \frac{\epsilon(1-|g|)}{2} |\psi_\theta^-\rangle\langle\psi_\theta^-| + O(\epsilon^2), \quad (5)$$

to the first order in ϵ, where $|\psi_\theta^{\pm}\rangle = (|0,1\rangle \pm e^{i\theta}|1,0\rangle)/\sqrt{2}$ and $\rho_{vac} = |0,0\rangle\langle0,0|$ in the photon-number basis. The first-order spatial coherence $g = |g|e^{i\theta}$, also known as the visibility, generally has an amplitude of $|g| \leq 1$. The nonlocal parity checks project onto the logical qubit states. After acting on $M \sim 1/\epsilon$ samples of ρ_{AB}, the memories likely contain one logical excitation. This postselection via measurement leads to efficient error accumulation, as elaborated on below. The visibility g can then be extracted through a logical measurement similar to the case of unary encoding discussed above [12].

Specifically, for the example of a photon being detected in the fifth time bin, the memory ends up in the following entangled state up to a known phase flip from the state transfer operation:

$$\frac{(1 \pm |g|)}{2} |\bar{\psi}_\theta^+\rangle\langle\bar{\psi}_\theta^+| + \frac{(1 \mp |g|)}{2} |\bar{\psi}_\theta^-\rangle\langle\bar{\psi}_\theta^-|, \quad (6)$$

where $|\bar{\psi}_\theta^\pm\rangle = (|\bar{0}, \bar{1}_5\rangle \pm e^{i\theta}|\bar{1}_5, \bar{0}\rangle)/\sqrt{2}$, which has four entangled physical qubits $(|00, 11\rangle \pm e^{i\theta}|11, 00\rangle)/\sqrt{2}$. The other even-parity qubits are in the $|0\rangle$ state and can be traced out. After measuring the first three of the four entangled qubits in the X basis, the remaining qubit is in the state

$$\frac{1}{2}[|0\rangle\langle0| + |1\rangle\langle1| + (-1)^{n_-}(g|0\rangle\langle1| + \text{H.c.})], \quad (7)$$

where n_- is the number of $|-\rangle$ outcomes from the X-basis measurements. Assume $n_- = 0$ for simplicity. Applying a phase shift of $U_\delta = |0\rangle\langle0| + e^{i\delta}|1\rangle\langle1|$ and measuring the qubit in the X basis will have outcome $|\pm\rangle$ with probability $[1 \pm \text{Re}(ge^{-i\delta})]/2$. The visibility g can then be extracted by sweeping over δ and repeating the above procedure for many photons.

Physically, our scheme can be implemented with long-lived atomic ground states (such as in Rb atoms) [37], solid-state qubits with an optical interface (such as SiV defect centers in diamond [38–40]), or spin qubits in quantum dots [41], which have fast control. Optical cavities ensure strong light-matter interaction [42], which is potentially matched via quantum frequency conversion [43]. Absorption of the photon by an auxiliary atom in a Raman setup [44,45] enables easy X-basis measurement, with the same atom reused for every optical mode. Maintaining a stable phase at the level specified by detector bandwidth can be accomplished with a reference laser, as done in atomic clocks [46]. Logical CX gates between the auxiliary atom and the memory atoms could be realized as cavity-mediated [47] or Rydberg gates [48]. Alternative schemes involve photon-atom gates [11,49] and photon detection, eliminating the auxiliary atom [43].

The dominant errors in our protocol will arguably originate from the two-qubit gates. Note, however, that all time bins except the one containing the photon will result in trivial CX gates where the control qubit is in state $|0\rangle$. The trivial action of the CX should have an error rate less than $\epsilon(\log_2 1/\epsilon)^{-1}$ to preserve the memory. A number of gate schemes satisfy this criterion [12]; for example, in photon-atom gates, the absence of a photon does not affect the atom. We therefore assume that only the nontrivial CX operations lead to significant errors. We also consider higher-order corrections to the photonic density matrix in Eq. (5), which introduce multiple-photon events leading to undetectable errors in the binary code.

The performance of our scheme is analyzed using the Fisher information, quantifying how much information about a given parameter can be extracted through measurement on a quantum state [50]. In our case, we wish to estimate the visibility $g = g_1 + ig_2$, where g_1 and g_2 are two real parameters, and so the Fisher information becomes a matrix. Taking the trace norm, $\|F\|$ quantifies the total obtainable information about g: $1/\|F\|$ has the operational interpretation of constraining the variance of the measured data [51]. Ideal nonlocal and local schemes operating on the state of Eq. (5) are separated by $\|F\| \geq M\epsilon$ and $\|F\| \leq M\epsilon^2$, respectively [6]. Intuitively, the nonlocal bound corresponds to the probability of detecting a photon from a source of intensity ϵ, whereas the local bound is a factor of ϵ worse due to the inability to discriminate against the vacuum component of the state. Thus, the Fisher information explicitly demonstrates how nonlocal schemes like ours are superior to local schemes like heterodyne detection for measuring weak thermal light, as found in the optical domain.

Incorporating errors and operating over M time bins, we find the following norm of the Fisher information, which is bounded from below [12]:

$$\|F\| \geq \frac{(M\epsilon)^2}{[(1+\epsilon)^M - 1](1+\epsilon)^{M+2}}\mu^2\nu^{\log_2(M+1)}$$

$$\equiv \|F\|_{\min}, \quad (8)$$

where $\mu \equiv p_t(2f_t - 1)^2(2f_1 - 1)^2$ contains the error in mapping the photonic state to memory at one site, in terms of the success probability p_t and fidelity f_t of the
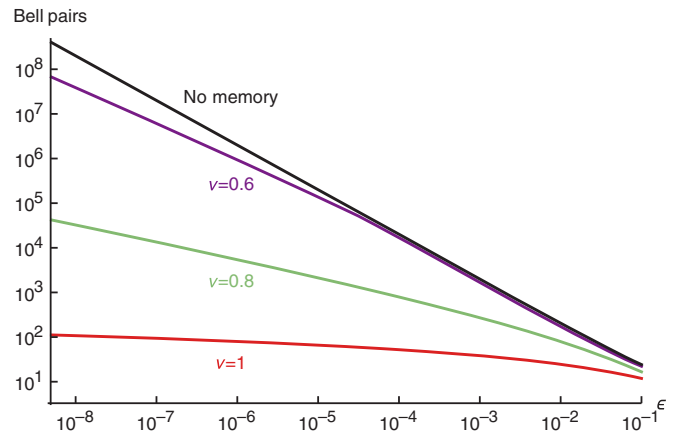

FIG. 2. Minimum number of Bell pairs needed to attain $\|F\| \geq 1$, corresponding to variance of $\lesssim 1$ in estimating the visibility g as a function of source intensity ϵ. We consider errors in the coding operations parametrized by decreasing ν, as detailed in the main text. Ideally ($\nu = 1$), $M \sim 1/\epsilon$ time bins are encoded per block and read out with $\log_2(M + 1)$ entangled pairs. For sufficiently large errors ($\nu = 0.6$), the encoding fails and memoryless operation with the readout of every time bin is recovered, similar to the scheme of Ref. [10].

light-memory transfer and of the one-qubit measurement f_1, and $\nu \equiv (2f_1 - 1)^4 (2f_2 - 1)^4 (2f_e - 1)$ contains the error of memory coding and readout in terms of the fidelities of one-qubit measurements f_1, nontrivial two-qubit gates f_2, and preshared entanglement f_e. The success probability includes photon loss, which effectively increases the vacuum component of the state. Other errors are not detectable and are modeled as depolarizing channels as a worst-case scenario. Note that $\|F\|_{\min} \sim M\epsilon$ for small ϵ, as expected for a nonlocal scheme. A larger M improves the probability of receiving the signal of a single photon, and hence $\|F\|_{\min}$ initially increases; eventually, however, a maximum is reached due to competition from multiple-photon events and imperfect quantum operations. Therefore, the scheme can be optimized with respect to M, operating with the minimum entanglement expenditure needed to extract the information content of one photon: $\|F\|_{\min} \geq 1$ (see Fig. 2). In the ideal case ($\nu = 1$), the number of entangled pairs is logarithmic in $1/\epsilon$, which is the number of time bins operated over so that roughly one photon arrives, on average. Information-theoretic arguments, based on the conditional entropy of the state described by Eq. (5), predict a bound with the same scaling, within a constant prefactor [12]. When errors are sufficiently large ($\nu \approx 60\%$), the memories are read out after a single time bin. Thus, an effective memoryless scheme similar to that of Ref. [10] is recovered, with entanglement consumption scaling as $1/\epsilon$ [53].

Assuming an effective detection bandwidth of $\delta_f = 10$ GHz, a total area of photon collection of 10 m^2, and imaging in the V band (centered around 555 nm), we can estimate the resources needed for a star of magnitude 10 (corresponding to $\epsilon = 7 \times 10^{-7}$), which is around the limit of the Center for High Angular Resolution Astronomy (CHARA) optical interferometric array [54]. Our ideal, optimized scheme requires $\log_2 1/\epsilon \sim 20$ memory qubits per site and an entanglement distribution rate of $\delta_f \epsilon \log_2 1/\epsilon \sim 200$ kHz [55]. The improvement over the rate necessary for a memoryless scheme [10] with the 10 GHz effective bandwidth is a factor of 5×10^4. Extending the current limit of the 330 m baseline of CHARA [56] to realistic quantum network scales greater than 10 km would increase resolution from the milliarcsecond to the microarcsecond regime [12]. Finally, we note that the bandwidth of direct interferometers can, in practice, be adjusted to enhance signal strength at the expense of resolution [56]. Although the present method is limited by the bandwidth of quantum memory, our approach readily extends to broadband operation, as discussed in Ref. [43].

Turning to possible implementations of these ideas, we note that the chosen detector bandwidth (10 GHz) sets the timescale of the encoding operation, and the photon arrival rate (1 kHz) determines the memory coherence time. In Table I of the Supplemental Material [12], we compare the capabilities of various physical realizations. Among the most promising candidates are SiV centers in diamond, striking a balance with the gate time on the order of

nanoseconds and millisecond-scale coherence. Techniques such as parallelization, repeated readout, and photon detection [43] improve performance with a modest overhead in resources. Furthermore, we emphasize that our scheme performs well in the presence of noise, which ultimately reduces the interference, as seen in Fig. 2. Therefore, it is amenable to experimental testing and development of noisy intermediate-scale quantum devices. Demonstrating kilohertz-scale entanglement generation between remote quantum memories, high-fidelity light-matter interfaces, and the addressing of multiple qubits at network nodes would facilitate the realization of our proposal.

In order to image a broad object, telescope arrays consisting of $N > 2$ sites are used to sample the visibility $g(x)$ across $N - 1$ points between $x = 0$ and $x = b$ (b is the baseline, or maximum length). According to the Van Cittert-Zernike theorem [57], a Fourier transform yields an estimate of the stellar intensity distribution $I(\phi)$. To operate in this manner, our network protocol generalizes to $N > 2$ nodes. Under conditions when one photon is incident on the telescope array, we encode the optical modes in a binary code, as in the two-node case. The nonlocal parity checks are performed using either N-qubit Greenberger–Horne–Zeilinger (GHZ) states, preserving coherence across the entire array, or with W states, collapsing the operation into pairwise readout [43]. Although a classical Fourier transform of extracted pairwise visibilities may be performed, the GHZ approach enables a quantum Fourier transform directly on the stored quantum state (see Fig. 3). Coherent processing of the visibilities in the latter case results in an
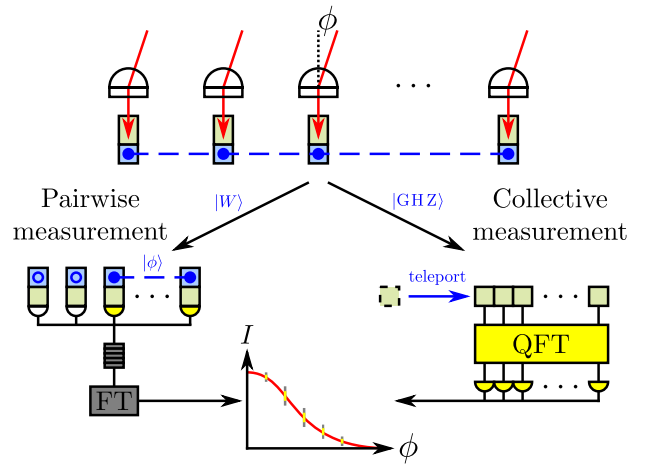

FIG. 3. Generalization to $N > 2$ sites in the telescope array. Decoding with a W state collapses the network state to two nodes, and the protocol continues as before. The visibility data are stored in a classical memory until enough events have accumulated to perform a Fourier transform (FT). Using GHZ states instead preserves coherence across the network. Quantum teleporting the memories to one site for convenience, a quantum Fourier transform (QFT) is applied, yielding the desired intensity distribution directly as the probabilities of measurement outcomes.

additional improvement in the signal-to-noise ratio because the noise associated with pairwise measurements is avoided. The exact improvement depends on the nature of the source distribution, but it can be on the order of $\sqrt{N}$ [43].

In conclusion, we have proposed a protocol for performing nonlocal interferometry over a quantum network, which is relevant for astronomical imaging. By encoding the quantum state of the incoming photons into memory, we realize an effective "event-ready" scheme with efficient entanglement expenditure. The nonlocality is vital for removing vacuum noise in imaging weak thermal light, and distributed entanglement circumvents transmission losses. Hence, our scheme enables near-term quantum networks to serve as a platform for powerful optical interferometers that are demonstrably superior to what can be achieved classically. Furthermore, quantum algorithms can be used to process the stored signals such that the stellar intensity distribution can be inferred with a further improvement in the signal-to-noise ratio.

Although we focused on addressing fundamental limitations, real-world interferometry suffers from many other practical challenges, such as stabilization and atmospheric phase fluctuations [5], which we address in Table II of the Supplemental Material [12]. For example, in Earth-based systems, atmospheric distortion can be tackled via a combination of adaptive optics and fringe tracking. Such techniques are already being deployed in smaller-scale astronomical interferometers [3] and are fully compatible with our proposal. Moreover, these challenges and control methods do not scale unfavorably with the baseline beyond certain physical correlation lengths [5], such that the construction of very large telescope arrays may be envisioned. Alternatively, space-based implementation avoids many of these technical issues, potentially extending over the 10^4 km scale [58] using entanglement distributed by satellites [59]. Because the astronomical origin of the weak thermal light is not crucial, such networks could also be applied to terrestrial imaging.

*Corresponding author.
ekhabiboulline@g.harvard.edu

[1] A. R. Thompson, Fundamentals of Radio Interferometry, in *Synthesis Imaging in Radio Astronomy II*, Astronomical Society of the Pacific Conference Series, Vol. 180, edited by G. B. Taylor, C. L. Carilli, and R. A. Perley (1999), p. 11.

[2] K. I. Kellermann and J. M. Moran, The development of high-resolution imaging in radio astronomy, Annu. Rev. Astron. Astrophys. **39**, 457 (2001).

[3] P. Stee *et al.*, Science cases for a visible interferometer, arXiv:1703.02395.

[4] T. A. ten Brummelaar, H. A. McAlister, S. T. Ridgway, J. W. G. Bagnuolo, N. H. Turner, L. Sturmann, J. Sturmann, D. H. Berger, C. E. Ogden, R. Cadman, W. I. Hartkopf, C. H. Hopper, and M. A. Shure, First results from the CHARA array. II. A description of the instrument, Astrophys. J. **628**, 453 (2005).

[5] A. R. Thompson, J. M. Moran, and G. W. Swenson, *Interferometry and Synthesis in Radio Astronomy*, 2nd ed. (Wiley-VCH Verlag GmbH, Weinheim, Germany, 2007).

[6] M. Tsang, Quantum Nonlocality in Weak-Thermal-Light Interferometry, Phys. Rev. Lett. **107**, 270402 (2011).

[7] P. Darré, R. Baudoin, J.-T. Gomes, N. J. Scott, L. Delage, L. Grossard, J. Sturmann, C. Farrington, F. Reynaud, and T. A. ten Brummelaar, First on-Sky Fringes with An Up-Conversion Interferometer Tested on a Telescope Array, Phys. Rev. Lett. **117**, 233902 (2016).

[8] H. J. Kimble, The quantum internet, Nature (London) **453**, 1023 (2008).

[9] H.-J. Briegel, W. Dür, J. I. Cirac, and P. Zoller, Quantum Repeaters: The Role of Imperfect Local Operations in Quantum Communication, Phys. Rev. Lett. **81**, 5932 (1998).

[10] D. Gottesman, T. Jennewein, and S. Croke, Longer-Baseline Telescopes Using Quantum Repeaters, Phys. Rev. Lett. **109**, 070503 (2012).

[11] S. Ritter, C. Nölleke, C. Hahn, A. Reiserer, A. Neuzner, M. Uphoff, M. Mücke, E. Figueroa, J. Bochmann, and G. Rempe, An elementary quantum network of single atoms in optical cavities, Nature (London) **484**, 195 (2012).

[12] See Supplemental Material at http://link.aps.org/supplemental/10.1103/PhysRevLett.123.070504 for details on the encoding map, derivation of the Fisher information, entanglement resource analysis, overview of technical specifications, and discussion of issues in realistic interferometry, along with Refs. [13–34].

[13] M. Horodecki, J. Oppenheim, and A. Winter, Partial quantum information, Nature (London) **436**, 673 (2005).

[14] M. Horodecki, J. Oppenheim, and A. Winter, Quantum state merging and negative information, Commun. Math. Phys. **269**, 107 (2006).

[15] C. Ahn, A. C. Doherty, P. Hayden, and A. J. Winter, On the distributed compression of quantum information, IEEE Trans. Inf. Theory **52**, 4349 (2006).

[16] I. Bjelaković, H. Boche, and G. Janßen, Universal quantum state merging, J. Math. Phys. (N.Y.) **54**, 032204 (2013).

[17] E. Waks, K. Inoue, and Y. Yamamoto, Multi-photon counting with visible light photon counter (VLPC), in *2002 Summaries of Papers Presented at the Quantum Electronics and Laser Science Conference* (Optical Society of America, 2002), pp. 29–30.

[18] J. Borregaard, P. Kómár, E. M. Kessler, A. S. Sørensen, and M. D. Lukin, Heralded Quantum Gates with Integrated Error Detection in Optical Cavities, Phys. Rev. Lett. **114**, 110502 (2015).

[19] R. Stockill, M. J. Stanley, L. Huthmacher, E. Clarke, M. Hugues, A. J. Miller, C. Matthiesen, C. Le Gall, and M. Atatüre, Phase-Tuned Entangled State Generation between Distant Spin Qubits, Phys. Rev. Lett. **119,** 010503 (2017).

[20] A. Reiserer, N. Kalb, G. Rempe, and S. Ritter, A quantum gate between a flying optical photon and a single trapped atom, Nature (London) **508,** 237 (2014).

[21] S. Welte, B. Hacker, S. Daiss, S. Ritter, and G. Rempe, Photon-Mediated Quantum Gate between Two Neutral Atoms in an Optical Cavity, Phys. Rev. X **8,** 011018 (2018).

[22] M. Körber, O. Morin, S. Langenfeld, A. Neuzner, S. Ritter, and G. Rempe, Decoherence-protected memory for a single-photon qubit, Nat. Photonics **12,** 18 (2018).

[23] D. Kim, S. G. Carter, A. Greilich, A. S. Bracker, and D. Gammon, Ultrafast optical control of entanglement between two quantum-dot spins, Nat. Phys. **7,** 223 (2011).

[24] L. Huthmacher, R. Stockill, E. Clarke, M. Hugues, C. Le Gall, and M. Atatüre, Coherence of a dynamically decoupled quantum-dot hole spin, Phys. Rev. B **97,** 241413(R) (2018).

[25] S. Sun, H. Kim, G. S. Solomon, and E. Waks, Cavity-Enhanced Optical Readout of a Single Solid-State Spin, Phys. Rev. Applied **9,** 054013 (2018).

[26] D. D. Sukachev, A. Sipahigil, C. T. Nguyen, M. K. Bhaskar, R. E. Evans, F. Jelezko, and M. D. Lukin, Silicon-Vacancy Spin Qubit in Diamond: A Quantum Memory Exceeding 10 ms with Single-Shot State Readout, Phys. Rev. Lett. **119,** 223602 (2017).

[27] R. E. Evans, M. K. Bhaskar, D. D. Sukachev, C. T. Nguyen, A. Sipahigil, M. J. Burek, B. Machielse, G. H. Zhang, A. S. Zibrov, E. Bielejec, H. Park, M. Lončar, and M. D. Lukin, Photon-mediated interactions between quantum emitters in a diamond nanocavity, Science **362,** 662 (2018).

[28] P. C. Maurer, G. Kucsko, C. Latta, L. Jiang, N. Y. Yao, S. D. Bennett, F. Pastawski, D. Hunger, N. Chisholm, M. Markham, D. J. Twitchen, J. I. Cirac, and M. D. Lukin, Room-temperature quantum bit memory exceeding one second, Science **336,** 1283 (2012).

[29] S. Lacour, F. Eisenhauer, S. Gillessen, O. Pfuhl, J. Woillez, H. Bonnet, G. Perrin, B. Lazareff, S. Rabien, V. Lapeyrère, Y. Clénet, P. Kervella, and Y. Kok, Reaching micro-arc second astrometry with long baseline optical interferometry: Application to the GRAVITY instrument, Astron. Astrophys. **567,** A75 (2014).

[30] S. T. Ridgway, *Visibility, Optical Tolerances, and Error Budget, Technical Report 2* (Center for High Angular Resolution Astronomy, Atlanta, GA, 1994).

[31] H. Bernien, B. Hensen, W. Pfaff, G. Koolstra, M. S. Blok, L. Robledo, T. H. Taminiau, M. Markham, D. J. Twitchen, L. Childress, and R. Hanson, Heralded entanglement between solid-state qubits separated by three metres, Nature (London) **497,** 86 (2013).

[32] H. Kaushal, V. K. Jain, and S. Kar, Free-space optical channel models, in *Free Space Optical Communication* (Springer India, New Delhi, 2017), p. 41.

[33] S. Muralidharan, L. Li, J. Kim, N. Lütkenhaus, M. D. Lukin, and L. Jiang, Optimal architectures for long distance quantum communication, Sci. Rep. **6,** 20463 (2016).

[34] B. Koehler, *VLTI Concept & Technical Aspects* (European Southern Observatory, Garching, 2001).

[35] J. Zmuidzinas, Cramér–Rao sensitivity limits for astronomical instruments: Implications for interferometer design, J. Opt. Soc. Am. A **20,** 218 (2003).

[36] M. Tsang, R. Nair, and X.-M. Lu, Quantum Theory of Superresolution for Two Incoherent Optical Point Sources, Phys. Rev. X **6,** 031033 (2016).

[37] H. P. Specht, C. Nolleke, A. Reiserer, M. Uphoff, E. Figueroa, S. Ritter, and G. Rempe, A single-atom quantum memory, Nature (London) **473,** 190 (2011).

[38] C. Wang, C. Kurtsiefer, H. Weinfurter, and B. Burchard, Single photon emission from SiV centres in diamond produced by ion implantation, J. Phys. B **39,** 37 (2006).

[39] L. J. Rogers, K. D. Jahnke, T. Teraji, L. Marseglia, C. Müller, B. Naydenov, H. Schauffert, C. Kranz, J. Isoya, L. P. McGuinness, and F. Jelezko, Multiple intrinsically identical single-photon emitters in the solid state, Nat. Commun. **5,** 4739 (2014).

[40] A. Sipahigil, K. D. Jahnke, L. J. Rogers, T. Teraji, J. Isoya, A. S. Zibrov, F. Jelezko, and M. D. Lukin, Indistinguishable Photons from Separated Silicon-Vacancy Centers in Diamond, Phys. Rev. Lett. **113,** 113602 (2014).

[41] D. Press, T. D. Ladd, B. Zhang, and Y. Yamamoto, Complete quantum control of a single quantum dot spin using ultrafast optical pulses, Nature (London) **456,** 218 (2008).

[42] A. Sipahigil, R. E. Evans, D. D. Sukachev, M. J. Burek, J. Borregaard, M. K. Bhaskar, C. T. Nguyen, J. L. Pacheco, H. A. Atikian, C. Meuwly, R. M. Camacho, F. Jelezko, E. Bielejec, H. Park, M. Lončar, and M. D. Lukin, An integrated diamond nanophotonics platform for quantum-optical networks, Science **354,** 847 (2016).

[43] See E. T. Khabiboulline, J. Borregaard, K. De Greve, and M. D. Lukin, companion paper, Quantum-assisted telescope arrays, Phys. Rev. A **100,** 022316 (2019) for extensions of our scheme that are relevant for a telescope array. We also provide details on the gain from a quantum Fourier transform and realizations of photon-memory state transfer.

[44] J. I. Cirac, P. Zoller, H. J. Kimble, and H. Mabuchi, Quantum State Transfer and Entanglement Distribution among Distant Nodes in a Quantum Network, Phys. Rev. Lett. **78,** 3221 (1997).

[45] A. D. Boozer, A. Boca, R. Miller, T. E. Northup, and H. J. Kimble, Reversible State Transfer between Light and a Single Trapped Atom, Phys. Rev. Lett. **98,** 193601 (2007).

[46] A. D. Ludlow, M. M. Boyd, J. Ye, E. Peik, and P. O. Schmidt, Optical atomic clocks, Rev. Mod. Phys. **87,** 637 (2015).

[47] T. Pellizzari, S. A. Gardiner, J. I. Cirac, and P. Zoller, Decoherence, Continuous Observation, and Quantum Computing: A Cavity QED Model, Phys. Rev. Lett. **75,** 3788 (1995).

[48] M. Saffman, T. G. Walker, and K. Mølmer, Quantum information with Rydberg atoms, Rev. Mod. Phys. **82,** 2313 (2010).

[49] T. G. Tiecke, J. D. Thompson, N. P. De Leon, L. Liu, V. Vuletic, and M. D. Lukin, Nanophotonic quantum phase switch with a single atom, Nature (London) **508,** 241 (2014).

[50] S. L. Braunstein and C. M. Caves, Statistical Distance and the Geometry of Quantum States, Phys. Rev. Lett. **72,** 3439 (1994).

[51] The Crámer-Rao bound [52] is $\Sigma \geq 1/F$, where Σ is the covariance matrix of the parameters being estimated. Note that $\|\Sigma\| \geq 1/\|F\|$ and the eigenvalues of Σ are the variances along the principal components of the measured data.

[52] C. W. Helstrom, Quantum detection and estimation theory, J. Stat. Phys. **1,** 231 (1969).

[53] *A priori*, there is a factor of 2 improvement from not having to postselect out half the photon events that do not reveal which-path information; our scheme always preserves coherence between sites. However, this advantage is counterbalanced by multiple-photon and gate errors.

[54] T. A. ten Brummelaar, J. Sturmann, S. T. Ridgway, L. Sturmann, N. H. Turner, H. A. McAlister, C. D. Farringtin, U. Beckmann, G. Weigelt, and M. Shure, The CLASSIC/CLIMB beam combiner at the CHARA array, J. Astron. Instrum. **02,** 1340004 (2013).

[55] Due to buildup of error, the optimized block length $1/\epsilon$ of encoded or decoded time bins decreases by a factor of (0.7,0.4,0.1) for $\nu \in (1, 0.8, 0.6)$. Also note that accounting for storing the preshared entangled pairs gives another factor of 2 for the memory requirement.

[56] E. Pedretti, J. D. Monnier, T. ten Brummelaar, and N. D. Thureau, Imaging with the CHARA interferometer, New Astron. Rev. **53,** 353 (2009), proceedings: VLTI summerschool.

[57] F. Zernike, The concept of degree of coherence and its application to optical problems, Physica (Utrecht) **5,** 785 (1938).

[58] J. D. Monnier, Optical interferometry in astronomy, Rep. Prog. Phys. **66,** 789 (2003).

[59] J. Yin *et al.*, Satellite-based entanglement distribution over 1200 kilometers, Science **356,** 1140 (2017).